

Electrostatic Measurements of Low Capacitance Changes in a Parallel Plate Capacitor

*Christian Sohl*¹, *Mats Gustafsson*¹, *Gerhard Kristensson*¹, *Davor Lovrić*¹, *Martin Nilsson*¹, and *Anders Sunesson*^{1,2}

¹ Dept. of Electrical and Information Technology, Lund University, P.O. Box 118, S-221 00 Lund, Sweden
{christian.sohl, mats.gustafsson, gerhard.kristensson}@eit.lth.se, citf.davor.lovric@gmail.com,
martin.nilsson@eit.lth.se

² Lite On Mobile, Science and Technology Park Ideon, S-223 70 Lund, Sweden
anders.sunesson@liteonmobile.com

Abstract

This paper describes an electrostatic experimental setup to measure the capacitance change when an uncharged object of arbitrary shape is inserted into a parallel plate capacitor. The employed measurement technique is discussed in detail, and measurements on two conducting spheres and two conducting circular cylinders of finite height are presented and compared with numerical simulations. It is concluded that the experimental setup is capable of detecting capacitance changes down to 10^{-17} F.

1 Introduction

This paper describes electrostatic measurements of the capacitance change when an uncharged object of arbitrary shape is inserted into a parallel plate capacitor. The present study is motivated by an interest to experimentally determine the electrostatic polarizability dyadic of an object, *i.e.*, the induced dipole moment when the object is immersed into a homogeneous electrostatic field of unit amplitude. The reason for this newborn interest in electrostatic quantities is because the electrostatic polarizability dyadic shows up in several intriguing sum rules as the fundamental quantity that relates the all-spectrum dynamic properties of certain electromagnetic problems to their electrostatic behavior. Sum rules on several such electromagnetic problems have been analyzed in the last couple of years and they include, but are not limited to, physical bounds on gain and bandwidth of single-port antennas, sum rules on broadband scattering, and transmission and reflection limitations on frequency selective surfaces and absorbers, respectively [2, 3, 5, 6]. In all these seemingly different electromagnetic problems, it has been shown that the electrostatic polarizability dyadic carries information on how well a design can be made and how far from optimal a given design is. In some cases, the electrostatic polarizability dyadic also gives insights into how a given design can be improved from an electromagnetic point of view. The sum rules are derived in a systematic way using analytic function theory and the assumptions of linearity, causality, and passivity. The general procedure to derive such sum rules is believed to be applicable to a wider class of electromagnetic problems than the ones discussed above.

The null-field approach can be utilized to solve for the change in capacitance and at the same time eliminate the higher order modes that are inevitable present due to the fact that the exciting sources in the parallel plate capacitor are located at a finite distance from the object [4]. The null-field approach applied to the parallel plate capacitor is reported in another paper at the same conference. The inverse problem of determining the electrostatic polarizability dyadic from successive electrostatic measurements of the capacitance change is also discussed in that reference. In particular, it is shown that the electrostatic polarizability dyadic can be found as the solution of an infinite-dimensional system of non-linear equations. This paper, however, focuses on the electrostatic experimental setup and the measurement technique employed for detecting low capacitance changes. The paper includes preliminary measurement results on conducting spheres and conducting circular cylinders of finite height. The inverse problem of determining the electrostatic polarizability dyadic from successive electrostatic measurements will be treated elsewhere.

Capacitance measurements can be divided into bridge comparison methods and time-constant methods [1, p. 129 and onwards]. Commercial instruments like LCR-meters often use bridge methods. The experimental setup described in this paper, however, uses a variant of a time-constant method where the measured capacitance is converted to a frequency. The reason for this choice of measurement technique is because it offers a wide dynamic range combined

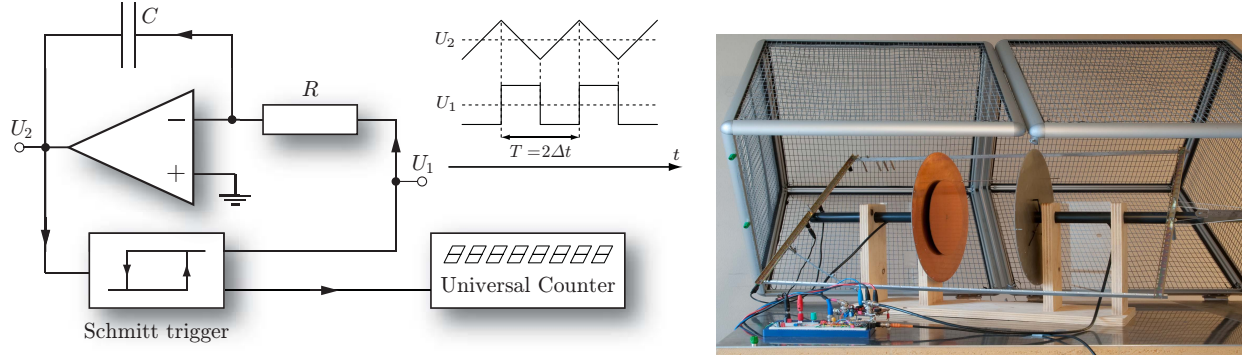


Figure 1: Block diagram of the operational amplifier circuit with voltage integrator, Schmitt trigger, and universal counter (left), and a photograph of the experimental setup (right).

with a good sensitivity. It fulfills the requirement to detect a low capacitance change against a background that is several orders of magnitude larger in capacitance.

2 Experimental Setup

A block diagram of the experimental setup is shown on the left-hand side of Figure 1. The experimental setup consists of a parallel plate capacitor with capacitance C (C denotes any of the capacitances C' and C'' defined in Section 3) and an operational amplifier circuit that converts C to a frequency with period time T . The parallel plate capacitor is used to set the frequency of an RC-oscillator. As long as the voltage U_2 in Figure 1 is not close to the supply voltage of the operational amplifier circuit, the integrator behaves like a linear time-invariant system:

$$\frac{dU_2}{dt} + \frac{1}{RC}U_1 = 0. \quad (1)$$

The Schmitt trigger is a voltage comparator with hysteresis which is described by the input-output relation in the block symbol on the left-hand side of Figure 1. Its output voltage U_1 is constant until U_2 reaches $-U_{\text{ref}}$ or $+U_{\text{ref}}$, where U_{ref} is an internal reference voltage. The voltage U_1 then switches to another constant voltage level where it remains until the other input limit is reached. This implies that U_1 becomes a square voltage wave as function of time. According to (1), the voltage U_2 is the time integral of U_1 . As a consequence, U_2 is a symmetrical triangle wave well within the linear region of the integrator. The slope of U_2 is set by $-U_1/(RC)$. Thus, the total integration time Δt when U_1 lies between $-U_{\text{ref}}$ and $+U_{\text{ref}}$ becomes independent of U_{ref} :

$$\Delta t = -\frac{\Delta U_2}{U_1}RC = -\frac{2U_{\text{ref}}}{-U_{\text{ref}}}RC = 2RC, \quad (2)$$

where $\Delta U_2 = 2U_{\text{ref}}$ is the voltage step of U_1 . The period time is therefore $T = 2\Delta t = 4RC$, or equivalently,

$$C = \frac{T}{4R}. \quad (3)$$

The experimental setup has been validated against a calibrated commercial LCR-meter, and the period time T is read by a universal counter. In this case a Jiwatsu SC-7201 with an accuracy better than 10^{-6} is used. In the experimental setup a $250 \text{ M}\Omega$ precision resistor is used and the reference voltage is chosen to be $U_{\text{ref}} = 5 \text{ V}$.

The parallel plate capacitor consists of two identical conducting circular plates of fixed radii $b = 11.0 \text{ cm}$ separated by a variable distance d . The electrostatic field is uniform near the axis of symmetry of the two plates provided $d/b \ll 1$. The experimental setup is shielded from outside disturbances by the means of a Faraday cage and a second pair of conducting circular plates with radii 19.2 cm positioned at the distance 0.8 cm behind the inner plates. The photograph on the right-hand side in Figure 1 shows the experimental setup with the Faraday cage opened. Its floor is

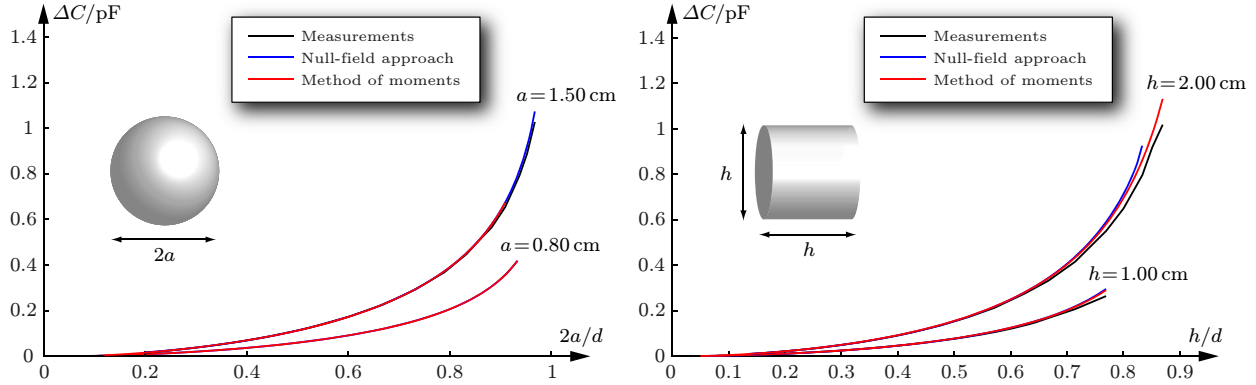


Figure 2: The change in capacitance ΔC for a conducting sphere of radius a (left) and a circular cylinder of radius $h/2$ and height h (right). Electrostatic measurements using the experimental setup described in Section 2 are compared to numerical simulations using the null-field approach and the method of moments.

made of solid aluminium, and wire netting in the walls and roof is connected to the circuit ground. The readout of d has an accuracy better than 0.5 mm, and capacitance values that can be measured with this experimental setup are in the range 1 pF to 100 pF. With good electrical screening we get a resolution of about 10^{-17} F for small C values.

3 Results and Discussion

The change in capacitance ΔC is defined as the difference of the capacitance C'' of the parallel plate capacitor with an uncharged object between the plates and the capacitance C' of the undisturbed parallel plate capacitor, *i.e.*,

$$\Delta C = C'' - C'. \quad (4)$$

The change in capacitance ΔC in units of 1 pF is depicted in Figure 2 as a function of the reciprocal value of the plate separation d for two conducting spheres and two conducting circular cylinders of finite height. The spheres have radii $a = 0.80$ cm and $a = 1.50$ cm, respectively, and the circular cylinders with radius $h/2$ and height h are characterized by $h = 1.00$ cm and $h = 2.00$ cm, respectively. Both the spheres and the circular cylinders were centered between the plates at the time of the measurement. Furthermore, the circular cylinders were oriented such that its axes of symmetry were aligned with the axis of symmetry of the experimental setup. From the left-hand side of Figure 2 it is seen that for a given value of d/a the capacitance change ΔC is largest for the sphere with the largest radius a . As expected, this implies that, for a fixed distance d between the plates, ΔC is largest for the sphere with the largest radius. The same conclusion holds for the circular cylinders on the right-hand side of Figure 2.

Figure 2 also contains numerical simulations using the null-field approach and the method of moments. From the figure it is seen that the measured results and the numerical simulations agree well for the spheres but show some discrepancies for large values of h/d for the circular cylinders. One possible reason for this discrepancy is the difficulty to align the cylinder between the plates for small plate separations. It is also seen that the two numerical methods deviate from each other for large values of h/d and a possible reason for this is the convergence problems in the null-field approach. Also the null-field approach assumes infinite plate radii and does not take into account the fringing effects of the parallel plate capacitor. In this respect, the numerical simulation for the circular cylinders based on the method of moments is believed to be more accurate than the corresponding result based on the null-field approach.

The experimental setup described in Section 2 is constrained in several ways, *e.g.*, by electrical noise and distance readout errors which limit the smallest plate separation that can be used. Electrical noise influences the electrostatic measurements in such a way that a small capacitance change becomes hard to detect with sufficiently high accuracy. An analysis of the influence of these and other types of constraints on the experimental setup will be treated in a

forthcoming paper.

4 Conclusions

It is concluded that the measurement setup described in this paper is capable of detecting capacitance changes down to 10^{-17} F. The measurement results show good agreement with the numerical simulations for conducting spheres and conducting circular cylinders of finite height. Other types of conducting objects and object with dielectric material parameters are currently under investigation. One difficulty using objects with no static conductivity is that the capacitance change becomes much smaller than the corresponding capacitance change for a conducting object with the same geometry. This motivates the need for higher accuracy in the experimental setup described in Section 2.

References

- [1] J. Bird. *Electrical circuit theory and technology*. Newnes Book Publishers, Oxford, second edition, 2003.
- [2] M. Gustafsson, C. Sohl, and G. Kristensson. Physical limitations on antennas of arbitrary shape. *Proc. R. Soc. A*, **463**, 2589–2607, 2007.
- [3] M. Gustafsson, C. Sohl, C. Larsson, and D. Sjöberg. Physical bounds on the all-spectrum transmission through periodic arrays. *EPL Europhysics Letters*, **87**(3), 34002 (6pp), 2009.
- [4] G. Kristensson. The polarizability and the capacitance change of a bounded object in a parallel plate capacitor. Technical Report LUTEDX/(TEAT-7203)/1–39/(2010), Lund University, Department of Electrical and Information Technology, P.O. Box 118, S-221 00 Lund, Sweden, 2010. <http://www.eit.lth.se>.
- [5] K. N. Rozanov. Ultimate thickness to bandwidth ratio of radar absorbers. *IEEE Trans. Antennas Propagat.*, **48**(8), 1230–1234, August 2000.
- [6] C. Sohl, M. Gustafsson, and G. Kristensson. Physical limitations on broadband scattering by heterogeneous obstacles. *J. Phys. A: Math. Theor.*, **40**, 11165–11182, 2007.